hydrogen

MDPI

Article

The Characteristics of a Ni/Cr/Ru Catalyst for a Biogas Dry Reforming Membrane Reactor Using a Pd/Cu Membrane and a Comparison of It with a Ni/Cr Catalyst

Akira Nishimura *, Mizuki Ichikawa, Souta Yamada and Ryoma Ichii

Division of Mechanical Engineering, Graduate School of Engineering, Mie University, Tsu 514-8507, Japan; 424m108@m.mie-u.ac.jp (M.I.); 423m161@m.mie-u.ac.jp (S.Y.); 424m107@m.mie-u.ac.jp (R.I.)
* Correspondence: nisimura@mach.mie-u.ac.jp; Tel.: +81-59-231-9747

Abstract: This study proposes a combination system consisting of a biogas dry reforming reactor and a solid oxide fuel cell (SOFC). Since biogas dry reforming is an endothermic reaction, this study adopted a membrane reactor operated due to the non-equilibrium state with H_2 separation from the reaction space. This study aimed to clarify the performance of the Ni/Cr/Ru catalyst using a biogas dry reforming membrane reactor. Additionally, this study also undertook a comparison of the performance of the Ni/Cr/Ru catalyst with that of the Ni/Cr catalyst. The impact of operation temperature, the molar ratio of CH_4:CO_2, the differential pressure between the reaction chamber and the sweep chamber, and the introduction of a sweep gas on the performance of the biogas dry reforming membrane reactor using a Pd/Cu membrane and a Ni/Cr/Ru catalyst was examined. The concentration of H_2 using the Ni/Cr/Ru catalyst was greater than that using the Ni/Cr catalyst by 2871 ppmV for the molar ratio of CH_4:CO_2 = 1.5:1 at the reaction temperature of 600 °C and the differential pressure of 0 MPa without a sweep gas in particular. Under this condition, CH_4 conversion, H_2 yield, and thermal efficiency were 67.4%, 1.77 × 10^{-2}%, and 0.241%, respectively.

Keywords: biogas dry reforming; membrane reactor; Ni/Cr/Ru catalyst; Ni/Cr catalyst; operation condition

Citation: Nishimura, A.; Ichikawa, M.; Yamada, S.; Ichii, R. The Characteristics of a Ni/Cr/Ru Catalyst for a Biogas Dry Reforming Membrane Reactor Using a Pd/Cu Membrane and a Comparison of It with a Ni/Cr Catalyst. *Hydrogen* **2024**, *5*, 414–435. https://doi.org/10.3390/hydrogen5030024

Academic Editor: Mihaela D. Lazar

Received: 30 April 2024
Revised: 21 June 2024
Accepted: 3 July 2024
Published: 10 July 2024

1. Introduction

Since H_2 is a secondary energy source, it is thought to be one of the promising fuels to solve the global warming problem around the world. Many countries including Japan are trying to develop technology in order to produce H_2 as well as systems using H_2 as a fuel. Though there are many approaches to producing H_2, this study focuses on biogas dry reforming to produce H_2. Generally, a biogas is a fuel consisting of CH_4 (55–75 vol%) and CO_2 (25–45 vol%) [1], which is generally produced from fermentation by the action of anaerobic microorganisms on raw materials, e.g., garbage, livestock excretion, and sewage sludge. In 2020, 1.46 EJ of produced biogas was obtained around the world, which was approximately five times higher than that produced in 2020 [2]. It can be expected that the amount of produced biogas will increase even more. Therefore, the authors of this study think that biogas will be a promising source to produce H_2.

Generally speaking, biogas is utilized as fuel for a gas engine or a micro gas turbine [3]. Biogas contains CO_2 of 40 vol% approximately, indicating that the efficiency of power generation is reduced because of the lower heating value compared with natural gas. We have already proposed a combination system consisting of a biogas dry reforming reactor and a solid oxide fuel cell (SOFC) [4–6]. The SOFC can use H_2 as well as CO, which is a by-product from biogas dry reforming, as a fuel. Therefore, the authors of this study think that this system could be used for a wider operation range than the proposed system.

Many studies have been conducted by researchers [7–13]. The selection of the catalyst used for biogas dry reforming is important. According to the literature survey by the

authors [7–11], the Ni-based catalyst is the most popular catalyst type for biogas dry reforming. Tang et al. developed [7] a Ni/Rh catalyst and revealed that the reaction of CH* → C* became more difficult to perform after the doping of Rh, which prevented the formation of C*. After that, the formation of carbon deposits was reduced, and the carbon deposition resistance of the Rh-Ni catalyst was improved. Ni/Al/LDF which was developed by Rosset et al. [8] performed CH_4 conversion of 88% and CO_2 conversion of 93% at the reaction temperature of 700 °C. Bimetallic Ni/Ru and Ni/Re catalysts developed by Moreno et al. [9] performed CH_4 conversion of 75% and CO_2 conversion of 82% at the reaction temperature of 1023 K. Ni-Ce/TiO_2-ZrO_2 developed by Shah and Modal [10] performed the maximum produced CH_4 of approximately 90% and H_2/CO ratio of 0.75 when the CO_2/CH_4 ratio was 1.5. Ni/CO/TiO_2 developed by Sharma and Dhir [11] performed CH_4 conversion of 87.13% and CO_2 conversion of 92.6% with 41.1% production of H_2. From the above literature survey, Ni alloy catalysts exhibit better performance in biogas dry reforming compared to pure Ni catalysts, e.g., due to the prevention of carbon deposition [7–11].

In addition, the Ru-based catalyst is also a popular catalyst type for biogas dry reforming. The Ru/ZrO_2-La_2O_3 catalyst developed by Soria et al. [12] induced an increase in CH_4 conversion and CO_2 conversion with temperature. CH_4 conversion and CO_2 conversion increased up to 25% and 20% at the reaction temperature of 500 °C, respectively. The Ru/Ni/Al_2O_3/$MgAl_2O_4$/YSZ catalyst developed by Andraos et al. [13] performed the CH_4 conversion of 96% and CO_2 conversion of 98% at 750 °C. The researchers investigated the effect of the molar ratio of CH_4:CO_2 on CH_4 conversion and CO_2 conversion; the highest CH_4 conversion and CO_2 conversion were obtained in the case of the molar ratio of CH_4:CO_2 = 1.6 and 1.8, respectively. The highest CH_4 conversion and CO_2 conversion were 56% and 20%, respectively.

Though several Ni-based bimetallic catalysts have been investigated, the Ni/Cr catalyst has not been investigated well other than in the authors' previous study [5]. In addition, there is no study on the characteristics of the Ni/Cr/Ru catalyst used for biogas dry reforming yet. Therefore, this study adopts the Ni/Cr/Ru catalyst for biogas dry reforming in order to clarify the performance of the Ni/Cr/Ru catalyst. In addition, this study compares the performance of the Ni/Cr/Ru catalyst used for biogas dry reforming with that of the Ni/Cr catalyst used for biogas dry reforming.

In addition, it is important to operate at a lower temperature for the improvement of the thermal energy efficiency of biogas dry reforming since biogas dry reforming is an endothermic reaction. For this purpose, the use of a membrane reactor is one effective procedure since H_2 production is promoted by providing the non-equilibrium state with H_2 separation from the reaction space [5]. Several Pd alloy membranes such as Pg/Ag and Pd/Au are commercialized as well as being used for research. However, the costs of Pd/Ag and Pd/Au, including pure Pd, are very expensive. On the other hand, the cost of Pd/Cu is relatively lower compared to Pd/Ag, Pd/Au, and pure Pd. To apply the system proposed by this study to the industry in the future, the cost is important. Therefore, we selected Pd/Cu as the H_2 separation membrane. According to the authors' previous study, the experimental investigation on the biogas dry reforming membrane reactor involved the use of a Pd/Cu membrane and Ni/Cr catalyst. Compared to the pure Ni catalyst, the concentration of produced H_2 was higher when using the Ni/Cr catalyst. There is no study to investigate the combination effect of the Ni/Cr (Ni/Cr/Ru) catalyst and a Pd/Cu membrane except for the authors' study, resulting in focusing on the benefits of using the Ni/Cr (Ni/Cr/Ru) catalyst and Pd/Cu membrane in this study.

The aim of this study was to clarify the performance of the Ni/Cr/Ru catalyst used for the biogas dry reforming membrane reactor. In addition, in this study, we also conducted a comparison of the performance of the Ni/Cr/Ru catalyst with that of the Ni/Cr catalyst. The impact of operation temperature, the molar ratio of CH_4:CO_2, the differential pressure between the reaction chamber and the sweep chamber, and the introduction of a sweep gas on the performance of the biogas dry reforming membrane reactor using a Pd/Cu

membrane and the Ni/Cr/Ru catalyst is examined. The molar ratio of CH_4:CO_2 = 1.5:1 simulates biogas in this study.

The reaction scheme of CH_4 dry reforming (DR) is described as follows:

$$CH_4 + CO_2 \leftrightarrow 2CO + 2H_2 + 247\ kJ/mol \quad (1)$$

Moreover, the following reaction schemes can be considered as the phenomena in this study:

$$CO_2 + H_2 \leftrightarrow CO + H_2O + 41\ kJ/mol \quad (2)$$

$$CO_2 + 4H_2 \leftrightarrow CH_4 + 2H_2O - 164\ kJ/mol \quad (3)$$

$$CH_4 + H_2O \leftrightarrow CO + 3H_2 - 41\ kJ/mol \quad (4)$$

where Equation (2) is a reverse water gas shift reaction (RWGS), Equation (3) is a methanation reaction, and Equation (4) is a steam reforming of CH_4. Regarding a carbon deposition, the following reaction scheme can be considered:

$$CH_4 \leftrightarrow C + 2H_2 + 75\ kJ/mol \quad (5)$$

$$2CO \leftrightarrow C + CO_2 - 173\ kJ/mol \quad (6)$$

$$CO_2 + 2H_2 \leftrightarrow C + 2H_2O - 90\ kJ/mol \quad (7)$$

$$CO + H_2 \leftrightarrow C + H_2O - 131\ kJ/mol \quad (8)$$

2. Experiment

2.1. Experimental Apparatus

Figure 1 illustrates the schematic drawing of the experimental apparatus of this study. The experimental apparatus consists of a gas cylinder, mass flow controllers (S48-32; HORIBA METRON INC. Beijing, China), pressure sensors (KM31), valves, a vacuum pump, a reactor composed of a reaction chamber and sweep chamber, and gas sampling taps. The reactor is installed in an electric furnace. The temperature in the electric furnace is controlled by far-infrared heaters (MCHNS1; MISUMI, Tokyo, Japan). CH_4 gas with a purity of over 99.4 vol% and CO_2 gas with a purity of over 99.9 vol% are controlled by the mass flow controllers and mixed before flowing into the reaction chamber. The pressure of the mixed gas at the inlet of the reaction chamber is measured by pressure sensors. Ar gas with a purity of over 99.99 vol% is controlled by a mass flow controller, and the pressure of Ar gas is measured by a pressure sensor. Ar is provided as a sweep gas. The exhausted gases at the outlet of the reaction chamber and sweep chamber are suctioned by a gas syringe via gas sampling taps. The concentration of sampled gas is measured using a TCD gas chromatograph (GL Science, Tokyo, Japan). The minimum resolution of the TCD gas chromatograph and the methanizer is 1 ppmV. The gas pressure at the outlet of the reactor is measured by a pressure sensor. The gas concentration and pressure are measured at the outlet of the reaction chamber and sweep chamber, respectively. The valve is installed at the outlet of the reaction chamber and it is closed when the reaction gas consisting of CH_4 and CO_2 flows into the reaction chamber. As a result, H_2 in the reaction chamber after contacting the Ni/Cr/Ru (Ni/Cr) catalyst penetrates the H_2 separation membrane and flows into the sweep chamber. In other words, no H_2 flows out of the reaction chamber unless it penetrates the H_2 separation membrane.

Figure 2 illustrates the details of the reactor in this study. The reactor is composed of a reaction chamber, a sweep chamber, and a H_2 separation membrane. The reaction chamber and the sweep chamber are made of stainless steel with the size of 40 mm × 100 mm × 40 mm. The volume of reaction space is 16×10^{-5} m^3. A porous Ni/Cr/Ru (Ni: 69.2 wt%, Cr: 29.6 wt%, Ru: 1.2 wt%) catalyst is charged in the reaction chamber. In addition, the Ni/Cr (Ni: 65 wt%, Cr: 35 wt%) catalyst is also charged in the reaction chamber as a reference catalyst. The mean hole diameter of the Ni/Cr/Ru catalyst and Ni/Cr catalyst is 1.95 mm.

From the manufacturer's brochure, the porosity of the Ni/Cr/Ru catalyst and Ni/Cr catalyst is 0.93. The weight of the charged Ni/Cr/Ru catalyst and Ni/Cr catalyst is 66.3 g and 55.3 g, respectively.

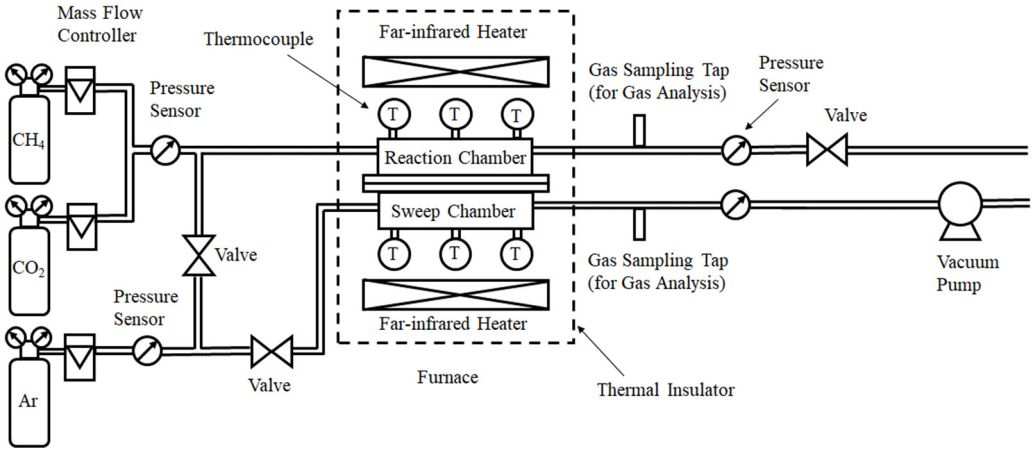

Figure 1. Schematic drawing of the experimental apparatus [5].

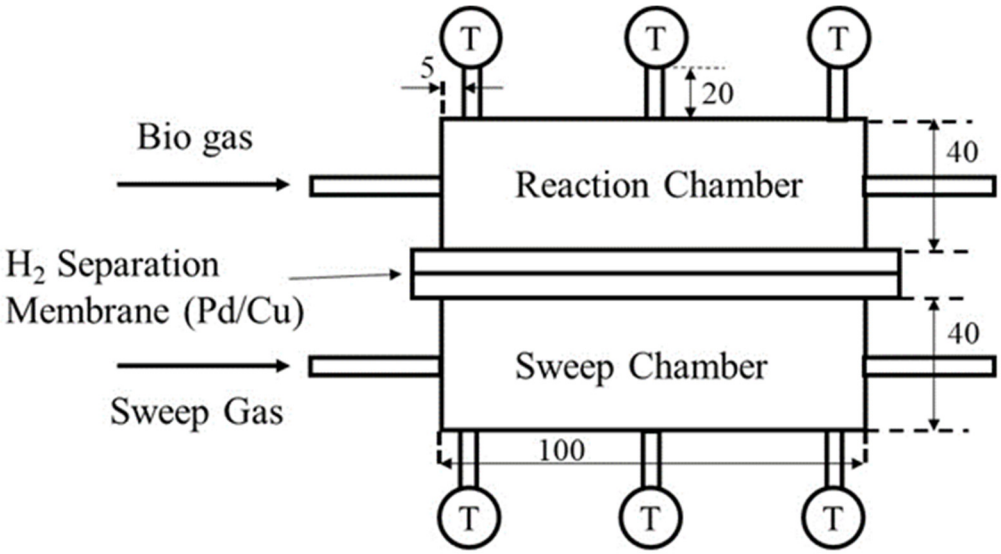

Figure 2. Schematic drawing providing details of the reactor part.

Figure 3 displays a photgraph of the catalyst filled in the reactor of this study. A Pd/Cu membrane (Cu of 40 wt%; Tanaka Kikinzoku, Tokyo, Japan) was selected as a H_2 separation membrane. The thickness of the Pd/Cu membrane is 20 µm. The temperatures at the inlet, the middle, and the outlet of the reaction and the sweep chamber are measured by K-type thermocouples. The initial reaction temperature is controlled and set by a far-infrared heater, which is confirmed by the thermocouples. The measured temperature and pressures are controlled by a data logger (GL240; Graphic Corporation, Tokyo, Japan).

Table 1 lists the experimental parameters in this study. The molar ratio of provided CH_4:CO_2 was changed by 1.5:1, 1:1, and 1:1.5. The molar ratio of CH_4:CO_2 simulates biogas in this study. According to the authors' previous study [14], the feed ratio of sweep gas to supply gas, which is defined as the flow rate of sweep gas divided by the flow rate of supply gas composed of CH_4 and CO_2, was set at 1.0, which is the optimum feed ratio of sweep gas to supply gas [14]. This study investigates the effect of the installation of sweep gas. To apply the system proposed by this study in industry, it is necessary to separate H_2 from the membrane reactor with a sweep gas and extract the H_2 from the sweep gas. Additional energy and equipment are necessary to install the system proposed by this

study in actual industry. On the other hand, if we can separate H_2 without a sweep gas from the membrane reactor, additional energy and equipment are not necessary. This is a merit of H_2 separation without a sweep gas. Therefore, this study performed a comparison of the presence vs. absence of sweep gas. The differential pressure between the reaction chamber and the sweep chamber was varied between 0 MPa, 0.010 MPa, and 0.020 MPa. This differential pressure is measured and confirmed by the pressure sensors installed at the outlet of the reaction chamber and the outlet of the sweep chamber. Regarding the differential pressure between the reaction chamber and the sweep chamber, in this study, we tried to conduct the experiment at a differential pressure of 0.030 MPa and a temperature of 600 °C. As a result, the Pd/Cu membrane was destroyed, e.g., a hole was made. Therefore, we report the results obtained at the differential pressure below 0.020 MPa in this study. The initial reaction temperature, which is the initial temperature of the reactor, is varied to 400 °C, 500 °C, and 600 °C. The initial reaction temperature is measured by thermocouples before flowing the mixed gas of CH_4 and CO_2 as well as the sweep gas into the reactor. During the experiment, the temperature of the reaction chamber decreased by approximately 3 °C due to the endothermic reaction, as listed above. In addition, in this study, we conducted a numerical simulation using the commercial software COMSOL Multiphysics with a 3D model including the simulation codes of the reaction as shown by Equations (1)–(6). In this numerical simulation, the distributions of each gas concentration, pressure, gas velocity as well as temperature were calculated. As a result, the temperature drops at the inlet, the middle, and the outlet of the reaction chamber on the center line are approximately 1 °C, 4 °C, and 1 °C, respectively. The gas concentrations at the outlet of the reaction chamber and the sweep chamber were detected using the FID gas chromatograph (GC320; GL Science) and methanizer (MT221; GL Science). This study shows the average data of five trials for each experimental condition in the following figures. The distribution of each gas concentration is below 10%.

Figure 3. Photograph of the charged Ni/Cr/Ru catalyst in the reactor.

Table 1. Parameters of the experimental conditions.

Parameters	Information
Initial reaction temperature (pre-set reaction temperature) [°C]	400, 500, 600
Pressure of supply gas [MPa]	0.10
Differential pressure between the reaction chamber and the sweep chamber [MPa]	0, 0.010 and 0.020
Molar ratio of provided CH_4:CO_2 (flow rate of provided CH_4:CO_2 [NL/min])	1.5:1, 1:1 and 1:1.5 (1.088:0.725, 0.725:0.725, 0.725:1.088)
Feed ratio of sweep gas to supply gas [-]	0 (W/O), 1.0 (W)

2.2. Assessment Factor to Evaluate the Performance of the Membrane Reactor

This study evaluates the performance of the proposed membrane reactor by examining gas concentration at the outlet of the reaction chamber and the sweep chamber. Using these data, CH_4 conversion (X_{CH_4}), CO_2 conversion (X_{CO_2}), H_2 yield (Y_{H_2}), H_2 selectivity (S_{H_2}), and CO selectivity (S_{CO}) were evaluated. These assessment factors are defined as follows:

$$X_{CH_4} = (C_{CH_4,\,in} - C_{CH_4,\,out})/(C_{CH_4,\,in}) \times 100 \quad (9)$$

$$X_{CO_2} = (C_{CO_2,\,in} - C_{CO_2,\,out})/(C_{CO_2,\,in}) \times 100 \quad (10)$$

$$Y_{H_2} = (1/2)(C_{H_2,\,out})/(C_{CH_4,\,in}) \times 100 \quad (11)$$

$$S_{H_2} = (C_{H_2,\,out})/(C_{H_2,\,out} + C_{CO,\,out}) \times 100 \quad (12)$$

$$S_{CO} = (C_{CO,\,out})/(C_{H_2,\,out} + C_{CO,\,out}) \times 100 \quad (13)$$

where $C_{CH_4,\,in}$ means the concentration of CH_4 at the inlet of the reaction chamber [ppmV], $C_{CH_4,\,out}$ means the concentration of CH_4 at the outlet of the reaction chamber [ppmV], $C_{CO_2,\,in}$ means the concentration of CO_2 at the inlet of the reaction chamber [ppmV], $C_{CO_2,\,out}$ is the concentration of CO_2 at the outlet of the reaction chamber [ppmV], $C_{H_2,\,out}$ means the concentration of H_2 at the outlet of the reaction chamber and sweep chamber [ppmV], and $C_{CO,\,out}$ means the concentration of CO at the outlet of the reaction chamber [ppmV].

Moreover, H_2 recovery (H) and permeation flux (F) are evaluated as follows:

$$H = (C_{H_2,\,out,\,sweep})/(C_{H_2,\,out,\,sweep} + C_{H_2,\,out,\,react}) \times 100 \quad (14)$$

$$F = \frac{P\left(\sqrt{P_{react,ave}} - \sqrt{P_{sweep,ave}}\right)}{\delta} \times 100 \quad (15)$$

where $C_{H_2,\,out,\,sweep}$ means the concentration of H_2 at the outlet of the sweep chamber [ppmV], $C_{H_2,\,out,\,react}$ means the concentration of H_2 at the outlet of the reaction chamber [ppmV], P means the permeation factor [mol/(m·s·$Pa^{0.5}$)], $P_{react,\,ave}$ means the average pressure of the reaction chamber [MPa], $P_{sweep,\,ave}$ means the average pressure of the sweep chamber [MPa], and δ means the thickness of the Pd/Cu alloy membrane [m].

Furthermore, the thermal efficiency of the membrane reactor (η) was also evaluated, which is defined as follows:

$$\eta = \frac{Q_{H_2}}{(W_{R.C.} + W_{S.C.} + W_p)} \times 100 \quad (16)$$

where Q_{H2} means the heating value of produced H_2 based on the lower heating value [W], $W_{R.C.}$ means the amount of pre-heat of supply gas for the reaction chamber [W], $W_{S.C.}$ means the amount of pre-heat of the sweep gas for the sweep chamber [W], and W_p is the pump power to give the differential pressure between the reaction chamber and the sweep chamber [W].

3. Results and Discussion

3.1. Comparison of Each Gas Concentration in the Reaction Chamber and Sweep Chamber Using the Ni/Cr/Ru Catalyst with That Using the Ni/Cr Catalyst When Changing the Reaction Temperature and the Differential Pressure between the Reaction Chamber and the Sweep Chamber

Figures 4 and 5 show the impact of reaction temperature on each gas concentration in the reaction chamber and the concentration of H_2 in the sweep chamber, respectively. The differential pressure between the reaction chamber and the sweep chamber was changed by 0 MPa, 0.010 MPa, and 0.020 MPa. In these figures, the molar ratio of CH_4:CO_2 is 1.5:1. In addition, W and W/O indicate the condition with a sweep gas and that without a sweep gas, respectively, in these figures. Each gas concentration in the reaction chamber and the sweep chamber using Ni/Cr/Ru catalyst was compared to that using Ni/Cr catalyst in these figures. Though this study shows the result of gas concentration in the unit of ppmV, it can be converted into the unit of mol. As to the gas concentration, 10,000 ppmV is 1 vol%. The gas volume can be calculated by multiplying the gas concentration by the volume of the reaction chamber, i.e., 40 mm × 100 mm × 40 mm or the volume of the sweep chamber, i.e., 40 mm × 100 mm × 40 mm. After that, the unit of gas volume, e.g., m^3 can be converted into mol by multiplying 22.4 kmol/m^3. Since the volume reaction chamber and sweep chamber and the conversion factor of 22.4 kmol/m^3 are constant, the authors of this study think that the gas concentration in the unit of ppmV can be used as an evaluation value for the performance of the reaction.

According to Figure 4, it can be seen that the concentration of H_2 in the reaction chamber increases with the increase in the reaction temperature. DR is an endothermic reaction, as shown in Equation (1), resulting in the reaction progressing well with the increase in the reaction temperature according to the theoretical kinetic study [15]. This tendency is confirmed irrespective of catalyst type as well as the differential pressure between the reaction chamber and the sweep chamber. On the other hand, it can be seen from Figure 5 that the concentration of H_2 in the sweep chamber increases with the increase in the reaction temperature. The concentration of H_2 in the reaction chamber is higher at higher reaction temperatures, resulting in the driving force to penetrate the Pd/Cu membrane being higher due to the high H_2 partial differential pressure between the reaction chamber and the sweep chamber, i.e., a high concentration difference in H_2 between the reaction chamber and the sweep chamber. As a result, a higher concentration of H_2 in the sweep chamber is obtained.

Regarding the impact of differential pressure between the reaction chamber and the sweep chamber, it is thought from Figures 4 and 5 that the concentration of H_2 in the reaction chamber and the sweep chamber is higher with the decrease in differential pressure. The authors think that the performance of the Ni/Cr/Ru (Ni/Cr) catalyst used in this study is not high since the reaction temperature is not high. Therefore, the reaction rate of the Ni/Cr/Ru (Ni/Cr) catalyst is lower compared to the H_2 separation rate of the Pd/Cu membrane relatively. If the H_2 separation rate of the Pd/Cu membrane is higher than the reaction rate of the Ni/Cr//Ru (Ni/Cr) catalyst, the effect of H_2 separation, which provides a non-equilibrium state in dry reforming, is not sufficiently effective. It is necessary to match the H_2 production rate of the Ni/Cr/Ru (Ni/Cr) catalyst and the H_2 separation rate of the Pd/Cu separation membrane in order to obtain the non-equilibrium state of dry reforming. Since the low H_2 separation rate might match the H_2 production rate of the Ni/Cr/Ru (Ni/Cr) catalyst in this study, the lower differential pressure provided better performance to obtain a higher concentration of H_2. As to the differential pressure of 0.020 MPa, the differential pressure is too high, resulting in the separation rate of H_2 possibly being higher than the production rate of H_2 in the reaction chamber. Since the permeation flux at the differential pressure of 0.020 MPa is 7.07×10^{-4} mol/(m^2·s), which is the highest among the investigated differential pressures, the effect of pressure on H_2 separation performance is the greatest. As a result, it is thought that the effective non-equilibrium state cannot be obtained. Comparing the concentration of H_2 in the reaction chamber shown in Figure 4, the concentration of H_2 at the differential pressure of 0.020 MPa is relatively lower than

that at the differential pressures. It was revealed that the production performance of H_2 is lower at the differential pressure of 0.020 MPa according to this tendency.

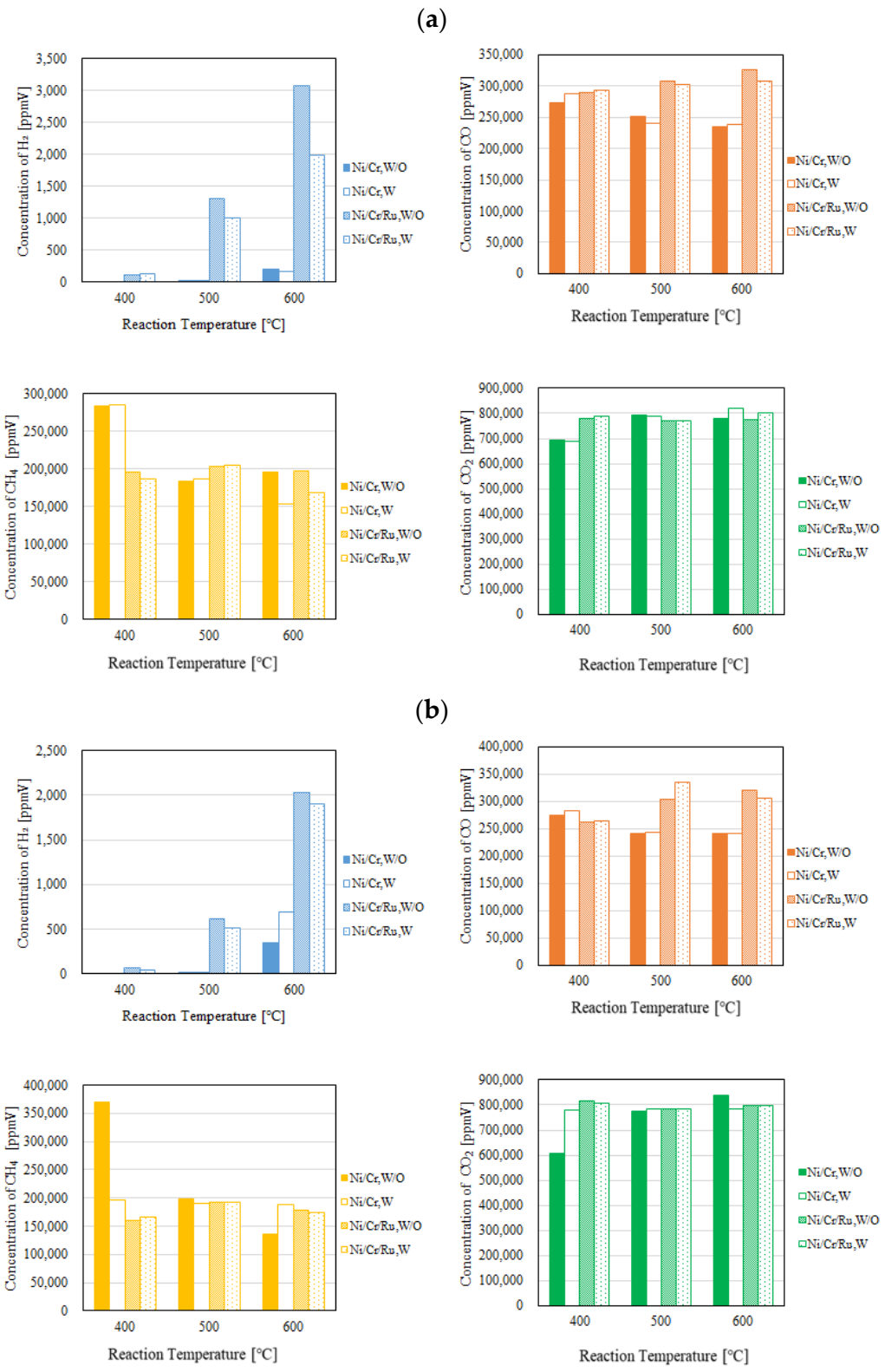

Figure 4. *Cont.*

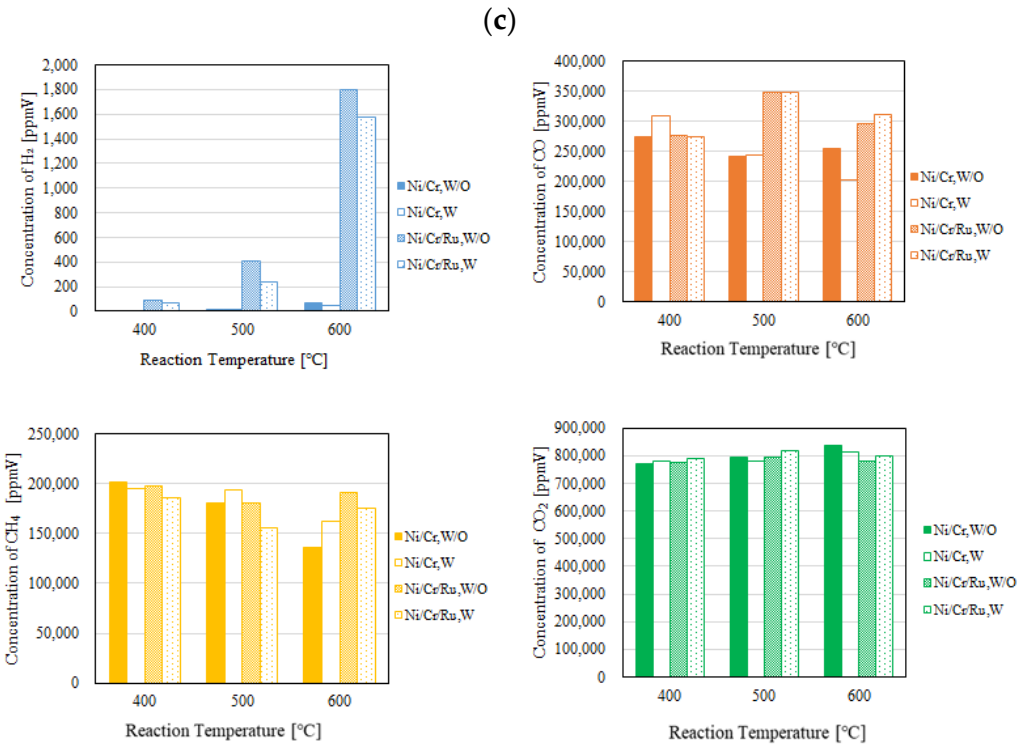

Figure 4. Comparison of each gas concentration in the reaction chamber using the Ni/Cr/Ru catalyst with the Ni/Cr catalyst reaction temperature changing (CH_4:CO_2 = 1.5:1, differential pressure: (**a**): 0 MPa, (**b**): 0.010 MPa, and (**c**): 0.020 MPa).

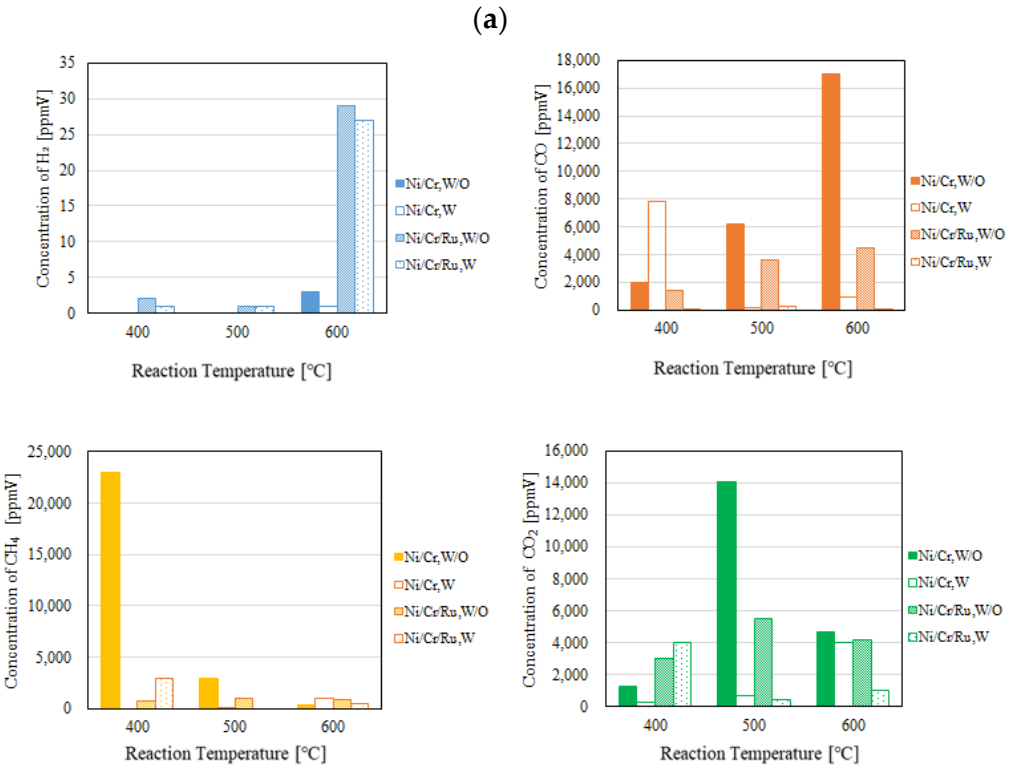

Figure 5. *Cont.*

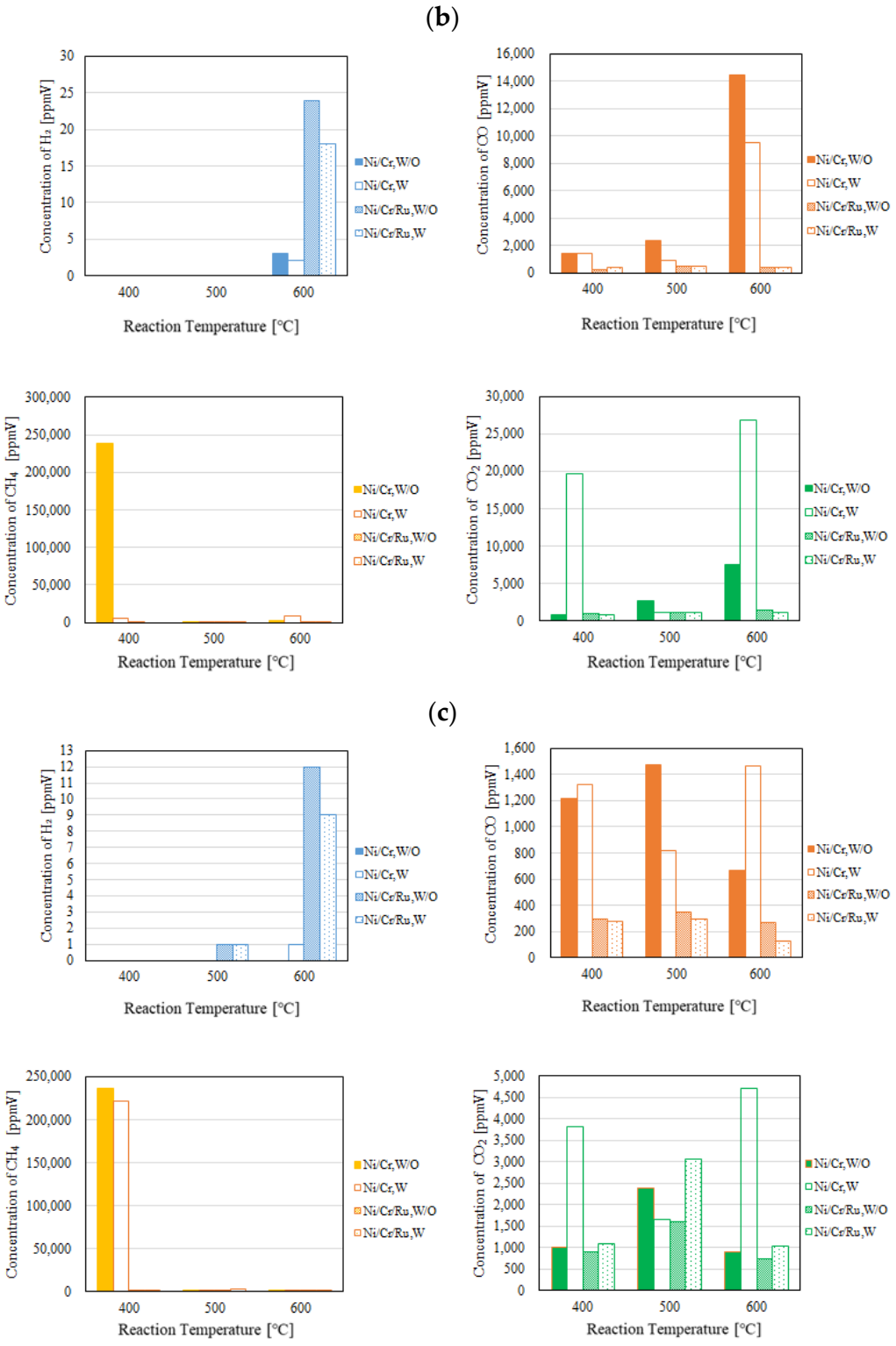

Figure 5. Comparison of each gas concentration in the sweep chamber using the Ni/Cr/Ru catalyst with the Ni/Cr catalyst reaction temperature changing (CH_4:CO_2 = 1.5:1, differential pressure: (**a**): 0 MPa, (**b**): 0.010 MPa, and (**c**): 0.020 MPa).

As to the impact of sweep gas, it is not significant according to Figures 4 and 5. Since the produced H_2 is not high, the driving force, i.e., the difference in the partial pressure of H_2 between the reaction chamber and the sweep chamber, is not high. As a result, it is

thought that the improvement in H_2 separation is not obtained by the introduction of the sweep gas.

Comparing the performance of catalyst type, the concentration of H_2 in the reaction chamber and that in the sweep chamber using the Ni/Cr/Ru catalyst are much higher than those using rg wNi/Cr catalyst according to Figures 4 and 5. This tendency is confirmed irrespective of the reaction temperature and the differential pressure. It is revealed in Figure 4 that the concentration of H_2 using the Ni/Cr/Ru catalyst is higher than that using the Ni/Cr catalyst by 2871 ppmV for the molar ratio of CH_4:CO_2 = 1.5:1 at the reaction temperature of 600 °C and the differential pressure of 0 MPa without a sweep gas in particular. Since there is no previous study investigating the performance of the Ni/Cr/Ru catalyst, this is new knowledge obtained in this study. According to a previous study investigating Ni/Ru/Al_2O_3, Ni/Ru/$MgAl_2O_4$, and Ni/Ru/YSZ [13], the supported material, e.g., $MgAl_2O_4$, having high sintering resistance played a very important role during the DR reaction. In addition, these supported materials exhibited significant interaction between Ni and them, resulting in high activity and stability. On the other hand, Cr was investigated as a co-catalyst in the authors' previous study [5]. We also reported that a decrease in carbon deposition due to the use of the Ni/Cr catalyst. As a result, it has been revealed that Ni/Cr is superior to Ni as a catalyst for biogas DR. In other words, Cr performs as a catalyst and does not perform as a supported material. In this study, Ni, Ru, and Cr were selected as catalysts. The authors of this study think that the synergy effect of them was obtained.

According to Figure 4, it can be seen that the concentration of CO is much higher than the concentration of H_2. According to the previous study using a Ni alloy catalyst, e.g., Ni/SiO_2 for biogas dry reforming [16], the H_2/CO ratio increases with the increase in reaction temperature up to 0.9 from 500 °C to 700 °C. In addition, from the previous study using a Ru alloy catalyst, e.g., Ru/MgAl for biogas dry reforming [17], the H_2/CO ratio increases with the increase in reaction temperature up to 0.4 from 550 °C to 650 °C. Therefore, the promotion of H_2 production can be expected over 600 °C. Since the Pd/Cu membrane (Cu: 40 wt%) cannot be used over 600 °C due to its durability, in this study, we did not conduct the experiment over 600 °C. In the near future, we would like to conduct the experiment over 600 °C after selecting the optimum H_2 separation membrane, i.e., composition and thickness.

3.2. Comparison of Each Gas Concentration in the Reaction Chamber and Sweep Chamber Using the Ni/Cr/Ru Catalyst with That Using the Ni/Cr Catalyst When Changing the Molar Ratio and the Differential Pressure between the Reaction Chamber and the Sweep Chamber

Figures 6 and 7 show the impact of the molar ratio on each gas concentration in the reaction chamber and the concentration of H_2 in the sweep chamber, respectively. The differential pressure between the reaction chamber and the sweep chamber was changed by 0 MPa, 0.010 MPa, and 0.020 MPa. In these figures, the reaction temperature is 600 °C. In addition, W and W/O indicate the condition with a sweep gas and that without a sweep gas, respectively, in these figures. Each gas concentration in the reaction chamber and the sweep chamber using the Ni/Cr/Ru catalyst is compared to that using the Ni/Cr catalyst in these figures.

It can be seen from Figure 6 that the highest concentration of H_2 is obtained for the molar ratio of CH_4:CO_2 = 1.5:1 at 600 °C irrespective of the differential pressure and the catalyst type. The tendency that the highest concentration of H_2 is obtained for the molar ratio of CH_4:CO_2 = 1.5:1 among the investigated molar ratios matches with the authors' previous study investigating Ni and Ni/Cr catalysts [5]. According to Figure 6, the concentration of H_2 in the reaction chamber is obtained in the case of a molar ratio of CH_4:CO_2 = 1.5:1 irrespective of catalyst type. The reaction mechanism to explain why the highest concentration of H_2 is obtained for the molar ratio of CH_4:CO_2 = 1.5:1 can be explained as follows [5]: since the amount of CH_4 is higher in this case, (i) H_2 is produced by the reactions shown in Equations (1) and (5), (ii) the produced H_2 is consumed by the reaction shown in Equation (2), resulting in CO production, (iii) a part of CO produced by

the reactions shown in Equations (1) and (2) is consumed by Equation (6), and (iv) H_2O produced by the reactions shown in Equations (2) and (3) is consumed during Equation (4).

According to Figure 7, the concentration of H_2 in the sweep chamber is the highest for the molar ratio of CH_4:CO_2 = 1.5:1 among the investigated molar ratios. The concentration of H_2 in the reaction chamber is higher at higher reaction temperatures, resulting in the driving force to penetrate the Pd/Cu membrane being greater due to the high H_2 partial differential pressure between the reaction chamber and the sweep chamber, i.e., a large concentration difference of H_2 between the reaction chamber and the sweep chamber. As a result, a higher concentration of H_2 in the sweep chamber is obtained.

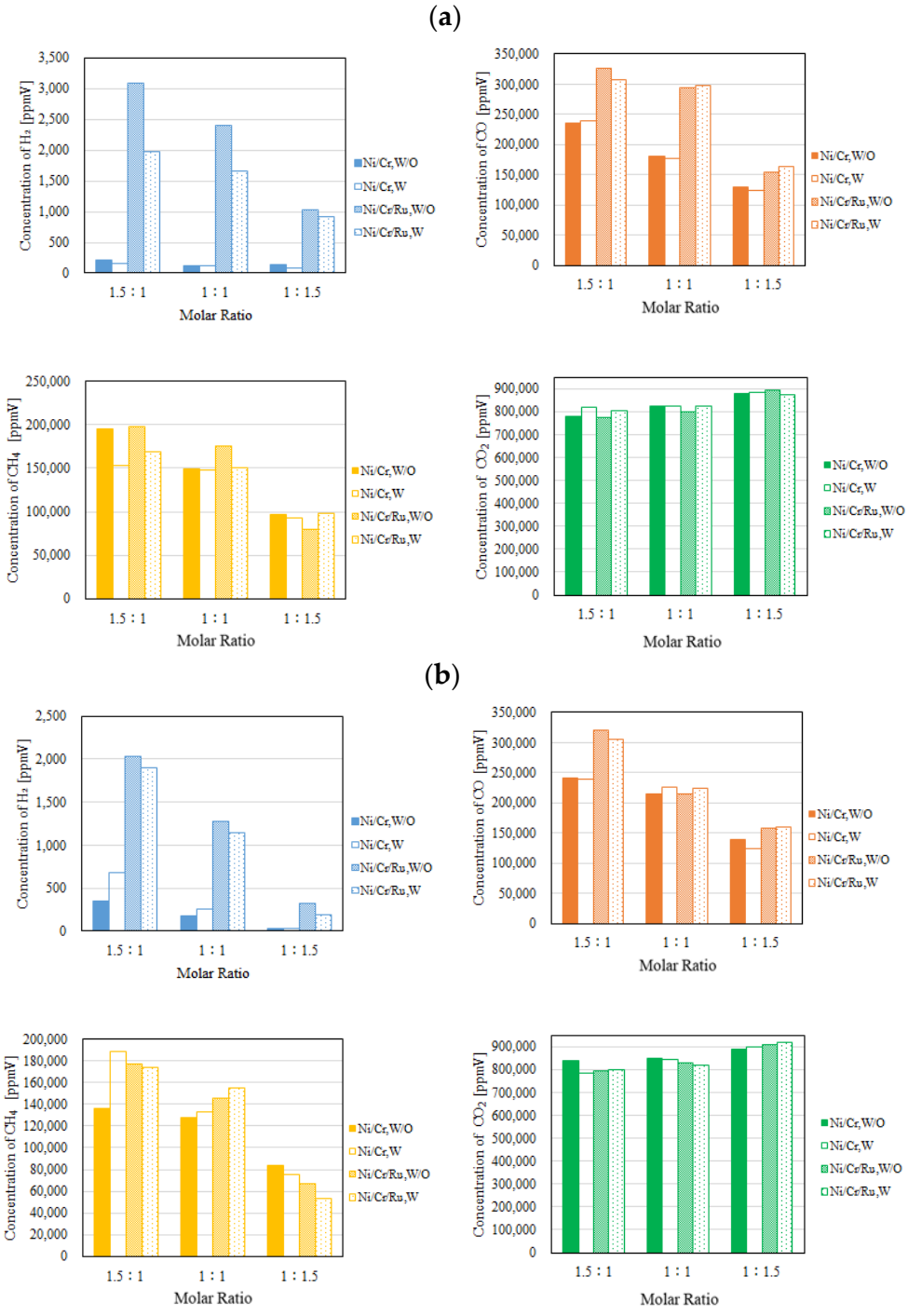

Figure 6. *Cont.*

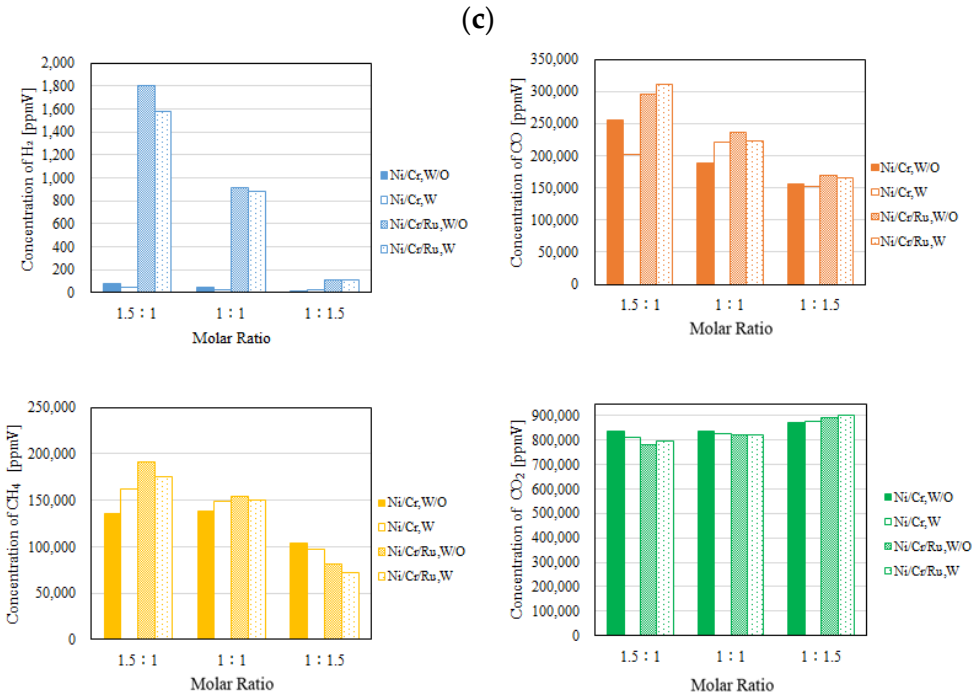

Figure 6. Comparison of each gas concentration in the reaction chamber using the Ni/Cr/Ru catalyst with the Ni/Cr catalyst molar ratio changing (CH_4:CO_2 = 1.5:1, differential pressure: (**a**): 0 MPa, (**b**): 0.010 MPa, and (**c**): 0.020 MPa).

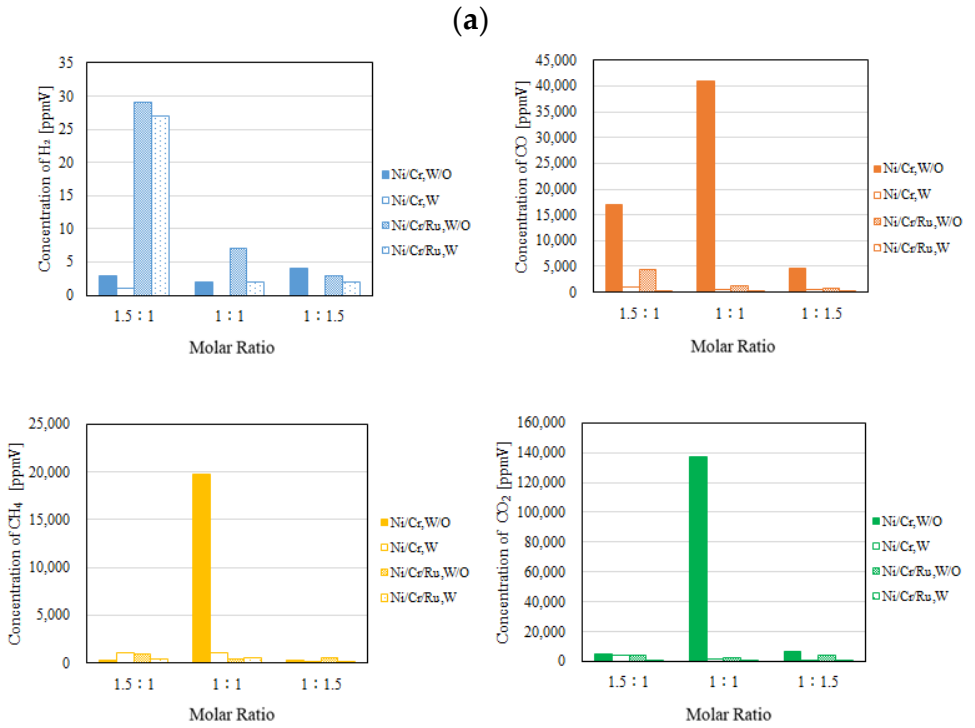

Figure 7. *Cont.*

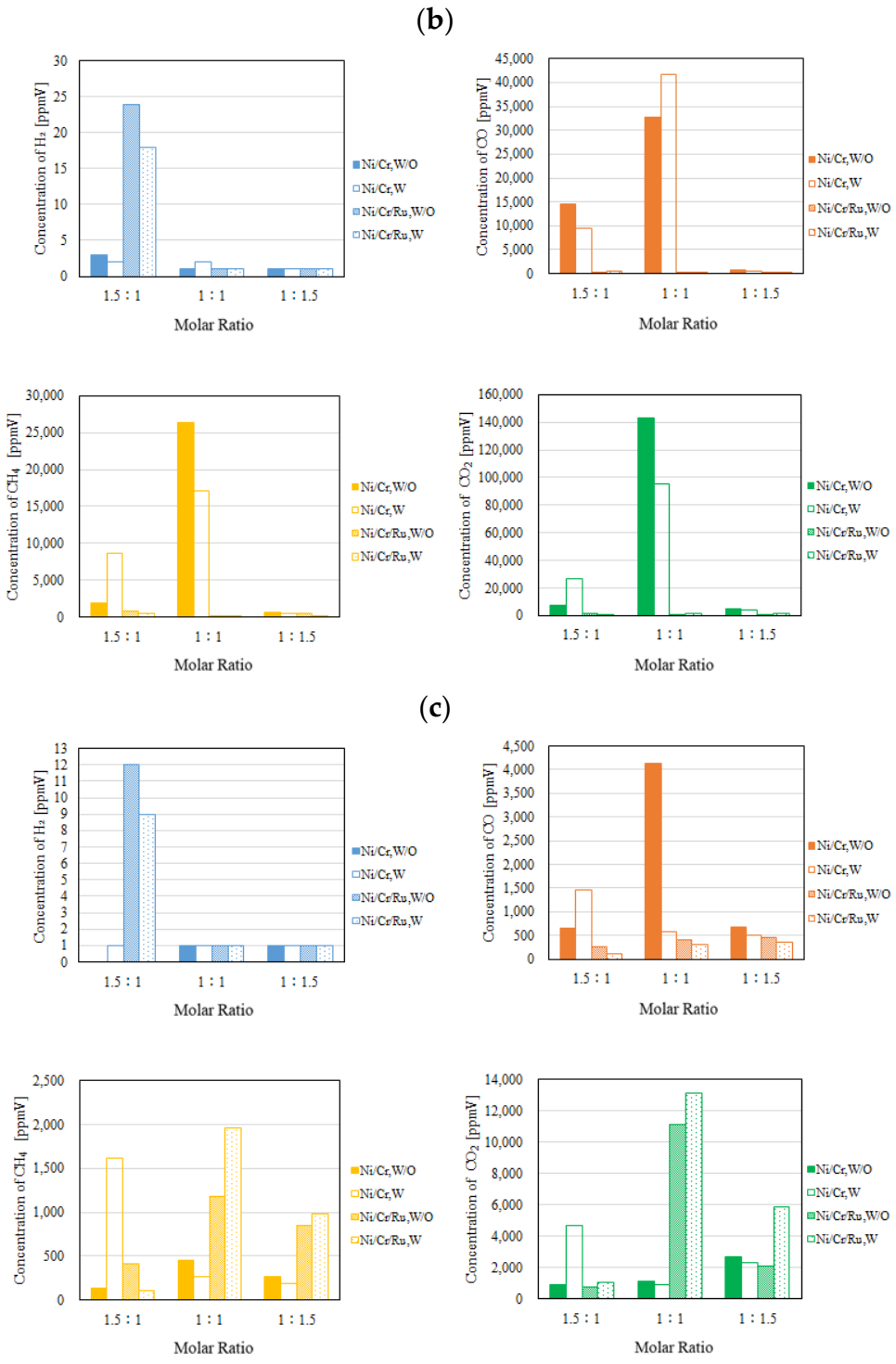

Figure 7. Comparison of each gas concentration in the sweep chamber using the Ni/Cr/Ru catalyst with the Ni/Cr catalyst molar ratio changing (CH_4:CO_2 = 1.5:1, differential pressure: (**a**): 0 MPa, (**b**): 0.010 MPa, and (**c**): 0.020 MPa).

According to Figures 4–7, the concentrations of CO, CH_4, and CO_2 are much higher than those of H_2 in the sweep chamber. The authors of this study think that the reactions that are shown by Equations (1)–(8) could have occurred in this study. In this study, the following reaction steps might have occurred:

(i) H_2 is produced by Equations (1) and (5).

(ii) The produced H_2 is consumed by Equations (2) and (3), resulting in CO, CH_4, and H_2O being produced.
(iii) The produced CO is consumed by Equations (6) and (8), resulting in C, CO_2, and H_2O being produced.

As a result, the authors of this study think that the concentration of CO, CH_4, and CO_2 is much higher than that of H_2 in the reaction chamber. Though Pd has the ability to extract H_2 preferentially, the Pd/Cu alloy might also penetrate the gas, except H_2, due to the rough crystal structure of the alloy compared to pure Pd. Since the difference in partial pressure of gas, i.e., the difference in the concentration of gas between the reaction chamber and the sweep chamber, is a driving force of gas penetration through the membrane, the authors of this study think that the concentration of CO, CH_4, and CO_2 is also higher than that of H_2 in the sweep chamber.

Comparing the performance of catalyst type, the concentration of H_2 in the reaction chamber and that in the sweep chamber using the Ni/Cr/Ru catalyst are much higher than those using Ni/Cr catalyst, especially for the molar ratio of CH_4:CO_2 = 1.5:1 according to Figures 6 and 7. It was revealed that the superiority of the Ni/Cr/Ru catalyst was obtained following the reaction mechanism as explained above. As to carbon deposition, which is explained by Equations (5) and (6), this was confirmed by the photographs shown in Figure 8. We can observe that the color of the catalyst changed to black, which indicates carbon deposition after the experiment. Regarding a carbon balance, this study did not measure the weight change of the catalyst per one experiment. This study measured the weight change of the catalyst after finishing all of the experiments shown in this paper. After all experiments including 108 experimental conditions were conducted, the weight of the Ni/Cr/Ru catalyst used in this study had increased by 0.1 g. Though the amount of produced carbon was small, carbon deposition was confirmed in this study. As to catalyst stability, the results of this study confirm that it did not change after conducting the experiments for approximately 250 h. Though coke formation was observed, the catalyst stability was kept due to there being no change in performance and durability. In addition, as to H_2O formation which is explained by Equations (2) and (3), this was confirmed by naked eye observation using a gas bag as shown in Figure 9. The methanizer and TCD gas chromatograph used for gas analysis in this study cannot detect H_2O since it is destroyed by absorbing H_2O on the surface of the column. Therefore, this study adopted a gas bag to capture H_2O exhausted from the reactor, which was installed at the outlet of the reactor. It is easy to observe the existence of H_2O with the naked eye due to the phase change from a gas into a liquid. The left figure in Figure 9 is the gas bag used to capture H_2O, which remains in the red circle shown in Figure 9. The changed color area on the white bar to capture H_2O, which is shown in the right figure in Figure 9, indicates the formation of liquid H_2O. The white bar shown in Figure 9 is used to show the existence of liquid H_2O. During the experiment, H_2O exists as a vapor since the reaction temperature is over 400 °C. After capturing H_2O using the gas bag, the phase of H_2O changes into a liquid due to a temperature drop. In addition, in this study, we conducted a numerical simulation by using the commercial software COMSOL Multiphysics with a 3D model including the simulation codes of the reactions as shown by Equations (1)–(6). In this simulation, the distributions of each gas concentration including H_2O, pressure, gas velocity, and temperature are calculated. As a result, the formation of H_2O was confirmed under several operating conditions, e.g., the molar ratio of CH_4:CO_2 = 1.5:1, the reaction temperature: 600 °C, and the differential pressure: 0 MPa (the concentration of H_2O of 0.2 mol/m^3). On the other hand, in this study, we did not measure the temperature drop due to the phase change of H_2O directly. The latent heat of H_2O during the phase change from a gas into a liquid is 1.96 MJ/Nm^3. Of note, 1 Nm^3 is equal to 1/22.4 kmol. Therefore, the latent heat of H_2O during the phase change from a gas into a liquid is 87.5 kJ/mol, i.e., 87.5 J/mol. On the other hand, as described above, the authors of this study think that the following reaction steps might have occurred:

(i) H_2 is produced by Equations (1) and (5).

(ii) The produced H_2 is consumed by Equations (2) and (3), resulting in CO, CH_4, and H_2O being produced.
(iii) The produced CO is consumed by Equations (6) and (8), resulting in C, CO_2, and H_2O being produced.

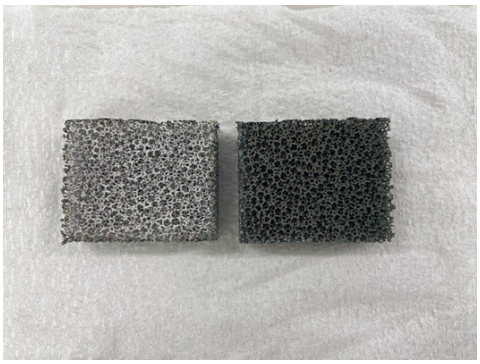

Figure 8. Photograph of the used catalyst (left: before the experiment; right: after the experiment).

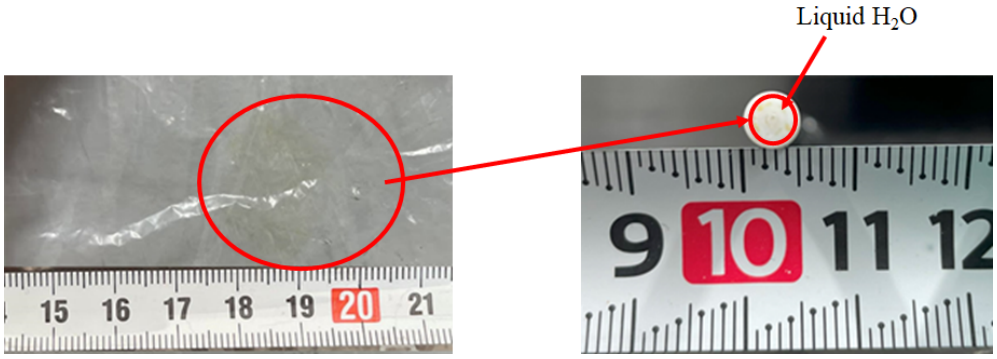

Figure 9. Photograph of the captured H_2O using the gas bag.

The latent heat of H_2O during the phase change from a gas into a liquid is very low compared to the enthalpy changes of Equations (1)–(3), (5), (6), and (8). Therefore, the authors of this study think the temperature drop due to the phase change of H_2O is small. On the other hand, during the experiment, the temperature of the reaction chamber decreased by approximately 3 °C due to endothermic reactions, which are listed above.

3.3. Comparison of the Assement Factors among the Investigated Experimental Conditions

To investigate the performance of the proposed membrane reactor using the Ni/Cu/Ru catalyst and the Pd/Cu membrane, Tables 2–4 list a comparison of CH_4 conversion, CO_2 conversion, H_2 yield, H_2 selectivity, CO selectivity, H_2 recovery, permeation flux and thermal efficiency for the different temperatures, the molar ratio of CH_4:CO_2, and the differential pressure between the reaction chamber and the sweep chamber. In these tables, the assessment factors for Ni/Cu are also listed as a reference.

It can be seen in Tables 2–4 that most of the CO_2 conversion shows a negative value. According to the concentrations of H_2, CH_4, and CO_2 shown in Figures 4–7 as well as CH_4 conversion and CO_2 conversion listed in Tables 2–4, a reaction consuming CH_4 and producing CO_2 occurs [5]. In addition, it can be seen from Tables 2–4 that the CO selectivity percentage is much higher than that for H_2 selectivity. Though H_2 is moved to the sweep chamber as shown in Figures 5 and 7, some H_2 that is produced remains in the reaction chamber as shown in Figures 6 and 8. Then, all of the H_2 produced does not move to the sweep chamber. Therefore, the reaction mechanism can be explained as follows [5]: (i) H_2 is produced by the reactions shown in Equations (1) and (5); (ii) the produced H_2 is consumed by the reaction shown in Equation (2), resulting in CO being produced; (iii) a part of CO produced by the reactions shown in Equations (1) and (2) is consumed during the reaction

shown in Equation (6); and (iv) H_2O produced during the reactions of Equations (2) and (3) is consumed by Equation (4). The production of carbon and H_2O was confirmed, as explained before.

Table 2. Comparison of CH_4 conversion, CO_2 conversion, H_2 yield, H_2 selectivity, CO selectivity, H_2 recovery, permeation flux, and thermal efficiency (pressure difference: 0 MPa; (**a**) CH_4:CO_2 = 1.5:1, (**b**) CH_4:CO_2 = 1:1, and (**c**) CH_4:CO_2 = 1:1.5).

Reaction Temperature [°C]	Catalyst	Sweep Gas	CH_4 Conversion [%]	CO_2 Conversion [%]	H_2 Yield [%]	H_2 Selectivity [%]	CO Selectivity [%]	H_2 Recovery [%]	Permeation Flux [mol/(m^2·s)]	Thermal Efficiency [%]
					(**a**)					
400	Ni/Cr	W/O	52.9	−73.0	0	0	100	0	0	0
		W	52.5	−72.5	0	0	100	0	0	0
	Ni/Cr/Ru	W/O	67.4	−94.8	1.03×10^{-2}	4.23×10^{-2}	100	1.63	0	0.213
		W	69.0	−97.2	1.05×10^{-2}	4.29×10^{-2}	100	0.794	0	0.141
500	Ni/Cr	W/O	69.3	−97.7	0	2.34×10^{-3}	100	0	0	8.36×10^{-3}
		W	68.9	−97.0	0	1.66×10^{-3}	100	0	0	3.55×10^{-3}
	Ni/Cr/Ru	W/O	66.2	−92.7	0	2.34×10^{-3}	100	0	0	8.36×10^{-3}
		W	65.7	−92.1	8.41×10^{-2}	0.332	99.7	9.91×10^{-2}	0	0.895
600	Ni/Cr	W/O	67.4	−94.9	1.77×10^{-2}	8.41×10^{-2}	99.9	1.42	0	0.241
		W	74.5	−105	1.33×10^{-2}	6.65×10^{-2}	99.9	0.625	0	0.117
	Ni/Cr/Ru	W/O	67.4	−94.9	1.77×10^{-2}	8.41×10^{-2}	99.9	1.42	0	0.241
		W	71.8	−101	0.167	0.649	99.4	1.34	0	1.46
					(**b**)					
400	Ni/Cr	W/O	55.0	−50.0	0	0	100	0	0	0
		W	63.7	−58.7	0	0	100	0	0	0
	Ni/Cr/Ru	W/O	66.9	−61.9	9.40×10^{-3}	4.26×10^{-2}	100	1.06	0	0.164
		W	70.0	−650.	7.50×10^{-3}	3.35×10^{-2}	100	1.33	0	8.31×10^{-2}
500	Ni/Cr	W/O	74.2	−69.2	0	0	100	0	0	0
		W	75.8	−70.8	0	0	100	0	0	0
	Ni/Cr/Ru	W/O	72.2	−67.0	6.22×10^{-2}	0.253	99.7	0.161	0	0.861
		W	72.7	−67.6	4.08×10^{-2}	0.171	99.8	0.245	0	0.360
600	Ni/Cr	W/O	70.3	−65.3	1.15×10^{-2}	5.17×10^{-2}	99.9	1.74	0	0.130
		W	69.8	−64.5	0.167	0.557	99.4	0.120	0	9.01×10^{-2}
	Ni/Cr/Ru	W/O	64.9	−59.4	0.241	0.812	99.2	0.290	0	2.76
		W	69.8	−64.5	0.167	0.557	99.4	0.120	0	1.22
					(**c**)					
400	Ni/Cr	W/O	79.4	−48.8	0	0	100	0	0	0
		W	79.5	−48.8	0	0	100	0	0	0
	Ni/Cr/Ru	W/O	77.4	−47.5	2.00×10^{-3}	1.14×10^{-2}	100	6.25	0	2.63×10^{-2}
		W	77.5	−47.5	2.38×10^{-3}	1.48×10^{-2}	100	0	0	2.13×10^{-2}
500	Ni/Cr	W/O	74.1	−45.2	0	0	100	0	0	0
		W	74.4	−45.4	0	0	100	0	0	0
	Ni/Cr/Ru	W/O	76.8	−47.0	2.06×10^{-2}	8.86×10^{-2}	99.9	0	0	0.229
		W	77.5	−47.5	1.30×10^{-2}	5.69×10^{-2}	99.9	0	0	9.21×10^{-2}
600	Ni/Cr	W/O	75.9	−46.4	1.70×10^{-2}	0.101	99.9	2.94	0	0.151
		W	76.9	−47.1	1.11×10^{-2}	7.16×10^{-2}	99.9	0	0	6.51×10^{-2}
	Ni/Cr/Ru	W/O	80.0	−49.0	0.129	0.660	99.3	0.291	0	1.18
		W	75.5	−46.0	0.116	0.561	99.4	0.216	0	0.677

Table 3. Comparison of CH_4 conversion, CO_2 conversion, H_2 yield, H_2 selectivity, CO selectivity, H_2 recovery, permeation flux, and thermal efficiency (pressure difference: 0.010 MPa; (**a**) CH_4:CO_2 = 1.5:1, (**b**) CH_4:CO_2 = 1:1, and (**c**) CH_4:CO_2 = 1:1.5).

Reaction Temperature [°C]	Catalyst	Sweep Gas	CH_4 Conversion [%]	CO_2 Conversion [%]	H_2 Yield [%]	H_2 Selectivity [%]	CO Selectivity [%]	H_2 Recovery [%]	Permeation Flux [mol/(m^2·s)]	Thermal Efficiency [%]
					(**a**)					
400	Ni/Cr	W/O	38.4	−51.3	0	0	100	0	5.00×10^{-3}	0
		W	67.2	−94.5	0	0	100	0	5.00×10^{-3}	0
	Ni/Cr/Ru	W/O	73.2	−104	5.92×10^{-3}	2.71×10^{-2}	100	0	5.00×10^{-3}	0.125
		W	72.2	−102	4.08×10^{-3}	1.84×10^{-2}	100	0	5.00×10^{-3}	5.51×10^{-2}
500	Ni/Cr	W/O	67.0	−94.2	0	1.23×10^{-3}	100	0	5.00×10^{-3}	4.18×10^{-3}
		W	68.2	−96.0	0	2.45×10^{-3}	100	0	5.00×10^{-3}	5.33×10^{-3}
	Ni/Cr/Ru	W/O	68.1	−95.7	5.12×10^{-2}	0.201	99.8	0	5.00×10^{-3}	0.856
		W	68.0	−95.6	4.27×10^{-2}	0.152	99.8	0	5.00×10^{-3}	0.455
600	Ni/Cr	W/O	77.4	−110	2.90×10^{-2}	0.136	99.9	0	5.00×10^{-3}	0.397
		W	68.5	−96.3	5.74×10^{-2}	0.275	99.7	0	5.00×10^{-3}	0.504
	Ni/Cr/Ru	W/O	70.4	−98.9	0.171	0.638	99.4	1.167	5.00×10^{-3}	2.34
		W	71.0	−99.8	0.160	0.624	99.4	0.938	5.00×10^{-3}	1.40
					(**b**)					
400	Ni/Cr	W/O	47.4	−42.4	0	0	100	0	5.00×10^{-3}	0
		W	26.8	−21.8	0	0	100	0	5.00×10^{-3}	0
	Ni/Cr/Ru	W/O	69.7	−64.7	7.80×10^{-3}	3.86×10^{-2}	100	0	5.00×10^{-3}	0.137
		W	72.7	−67.7	6.70×10^{-3}	3.34×10^{-2}	100	0	5.00×10^{-3}	7.53×10^{-2}
500	Ni/Cr	W/O	78.7	−73.7	0	1.66×10^{-3}	100	0	5.00×10^{-3}	4.16×10^{-3}
		W	81.6	−76.6	0	1.13×10^{-3}	100	0	5.00×10^{-3}	1.77×10^{-3}
	Ni/Cr/Ru	W/O	68.4	−63.3	4.44×10^{-2}	0.186	99.8	0	5.00×10^{-3}	0.616
		W	74.2	−69.1	3.68×10^{-2}	0.126	99.9	0	5.00×10^{-3}	0.326
600	Ni/Cr	W/O	74.5	−69.5	1.83×10^{-2}	7.41×10^{-2}	99.9	0.546	5.00×10^{-3}	0.209
		W	73.5	−68.4	2.60×10^{-2}	9.70×10^{-2}	99.9	0.769	5.00×10^{-3}	0.189
	Ni/Cr/Ru	W/O	70.8	−65.6	0.128	0.595	99.4	7.80×10^{-2}	5.00×10^{-3}	1.47
		W	68.9	−63.7	0.115	0.509	99.5	0.087	5.00×10^{-3}	0.841
					(**c**)					
400	Ni/Cr	W/O	97.4	−60.8	0	0	100	0	5.00×10^{-3}	0
		W	76.2	−46.6	0	0	100	0	5.00×10^{-3}	0
	Ni/Cr/Ru	W/O	76.9	−47.1	2.25×10^{-3}	1.21×10^{-2}	100	5.56	5.00×10^{-3}	2.98×10^{-2}
		W	74.3	−45.3	2.25×10^{-3}	1.22×10^{-2}	100	0	5.00×10^{-3}	2.02×10^{-2}
500	Ni/Cr	W/O	76.2	−46.6	0	0	100	0	5.00×10^{-3}	0
		W	77.0	−47.2	0	0	100	0	5.00×10^{-3}	0
	Ni/Cr/Ru	W/O	72.7	−44.3	1.46×10^{-2}	6.48×10^{-2}	99.9	0	5.00×10^{-3}	0.162
		W	75.4	−46.1	9.50×10^{-3}	4.12×10^{-2}	100	1.32	5.00×10^{-3}	6.64×10^{-2}
600	Ni/Cr	W/O	79.0	−48.5	3.75×10^{-3}	2.14×10^{-2}	100	3.33	5.00×10^{-3}	3.32×10^{-2}
		W	81.2	−50.0	3.50×10^{-3}	2.26×10^{-2}	100	3.57	5.00×10^{-3}	1.97×10^{-2}
	Ni/Cr/Ru	W/O	83.2	−51.2	4.01×10^{-2}	0.202	99.8	0.312	5.00×10^{-3}	0.366
		W	86.7	−53.6	2.34×10^{-2}	0.117	99.9	0.535	5.00×10^{-3}	0.136

Table 4. Comparison of CH_4 conversion, CO_2 conversion, H_2 yield, H_2 selectivity, CO selectivity, H_2 recovery, permeation flux, and thermal efficiency (pressure difference: 0.020 MPa; (**a**) CH_4:CO_2 = 1.5:1, (**b**) CH_4:CO_2 = 1:1, and (**c**) CH_4:CO_2 = 1:1.5).

Reaction Temperature [°C]	Catalyst	Sweep Gas	CH_4 Conversion [%]	CO_2 Conversion [%]	H_2 Yield [%]	H_2 Selectivity [%]	CO Selectivity [%]	H_2 Recovery [%]	Permeation Flux [mol/(m^2·s)]	Thermal Efficiency [%]
					(**a**)					
400	Ni/Cr	W/O	66.3	−93.2	0	0	100	0	7.07×10^{-3}	0
		W	67.6	−95.1	0	0	100	0	7.07×10^{-3}	0
	Ni/Cr/Ru	W/O	67.0	−94.2	7.08×10^{-3}	3.08×10^{-2}	100	0	7.07×10^{-3}	0.150
		W	68.9	−97.1	6.00×10^{-3}	2.63×10^{-2}	100	0	7.07×10^{-3}	8.08×10^{-2}
500	Ni/Cr	W/O	69.9	−98.6	0	1.64×10^{-3}	100	0	7.07×10^{-3}	5.57×10^{-3}
		W	67.7	−95.3	0	2.45×10^{-3}	100	0	7.07×10^{-3}	5.33×10^{-3}
	Ni/Cr/Ru	W/O	69.9	−98.5	3.40×10^{-2}	0.117	99.9	0.245	7.07×10^{-3}	0.567
		W	74.0	−105	1.97×10^{-2}	6.78×10^{-2}	99.9	0.424	7.07×10^{-3}	0.209
600	Ni/Cr	W/O	77.3	−110	6.17×10^{-3}	2.90×10^{-2}	100	0	7.07×10^{-3}	8.53×10^{-2}
		W	72.9	−103	4.33×10^{-3}	2.56×10^{-2}	100	1.92	7.07×10^{-3}	3.75×10^{-2}
	Ni/Cr/Ru	W/O	68.2	−95.6	0.151	0.611	99.4	0.661	7.07×10^{-3}	2.08
		W	70.8	−99.6	0.132	0.508	99.5	0.567	7.07×10^{-3}	1.16
					(**b**)					
400	Ni/Cr	W/O	67.2	−62.2	0	0	100	0	7.07×10^{-3}	0
		W	25.5	−20.5	0	0	100	0	7.07×10^{-3}	0
	Ni/Cr/Ru	W/O	72.9	−67.8	4.80×10^{-3}	2.37×10^{-2}	100	0	7.07×10^{-3}	8.46×10^{-2}
		W	74.4	−69.4	4.00×10^{-3}	1.87×10^{-2}	100	0	7.07×10^{-3}	4.49×10^{-2}
500	Ni/Cr	W/O	69.8	−64.8	0	4.32×10^{-3}	100	0	7.07×10^{-3}	1.39×10^{-3}
		W	69.4	−64.4	0	1.81×10^{-3}	100	0	7.07×10^{-3}	3.54×10^{-3}
	Ni/Cr/Ru	W/O	73.3	−68.2	3.47×10^{-2}	0.139	99.9	0	7.07×10^{-3}	0.481
		W	71.5	−66.4	2.79×10^{-2}	0.113	99.9	0.358	7.07×10^{-3}	0.246
600	Ni/Cr	W/O	72.3	−67.3	5.00×10^{-3}	2.59×10^{-2}	100	2.00	7.07×10^{-3}	5.63×10^{-2}
		W	70.1	−65.1	2.20×10^{-3}	9.92×10^{-3}	100	4.55	7.07×10^{-3}	1.54×10^{-2}
	Ni/Cr/Ru	W/O	69.1	−63.9	9.12×10^{-2}	0.384	99.6	0.110	7.07×10^{-3}	1.05
		W	69.9	−64.7	8.87×10^{-2}	0.396	99.6	0.113	7.07×10^{-3}	0.649
					(**c**)					
400	Ni/Cr	W/O	66.3	−93.2	0	0	100	0	7.07×10^{-3}	0
		W	67.6	−95.1	0	0	100	0	7.07×10^{-3}	0
	Ni/Cr/Ru	W/O	67.0	−94.2	7.08×10^{-3}	3.08×10^{-2}	100	0	7.07×10^{-3}	0.150
		W	68.9	−97.1	6.00×10^{-3}	2.63×10^{-2}	100	0	7.07×10^{-3}	8.09×10^{-2}
500	Ni/Cr	W/O	78.7	−48.3	0	0	100	0	7.07×10^{-3}	0
		W	81.1	−49.9	0	0	100	0	7.07×10^{-3}	0
	Ni/Cr/Ru	W/O	76.6	−46.9	1.19×10^{-2}	5.35×10^{-2}	99.9	1.05	7.07×10^{-3}	0.130
		W	78.0	−47.8	9.50×10^{-3}	4.02×10^{-2}	100	0	7.07×10^{-3}	6.73×10^{-2}
600	Ni/Cr	W/O	73.9	−45.1	2.25×10^{-3}	1.15×10^{-2}	100	5.56	7.07×10^{-3}	1.94×10^{-2}
		W	75.6	−46.2	3.88×10^{-3}	2.04×10^{-2}	100	3.23	7.07×10^{-3}	2.19×10^{-2}
	Ni/Cr/Ru	W/O	79.7	−48.9	1.41×10^{-2}	6.62×10^{-2}	99.9	0.885	7.07×10^{-3}	0.128
		W	81.8	−50.4	1.35×10^{-2}	6.51×10^{-2}	99.9	0.926	7.07×10^{-3}	7.82×10^{-2}

From the investigation in this study, the highest concentration of H_2 using the Ni/Cr/Ru catalyst was obtained for the molar ratio of CH_4:CO_2 = 1.5:1 at the reaction tempera-

ture of 600 °C and the differential pressure of 0 MPa without a sweep gas, which is 3080 ppmV. Under this condition, CH_4 conversion, H_2 yield, and thermal efficiency are 67.4%, 1.77×10^{-2}%, and 0.241%, respectively. This result is not high compared to previous studies using Ni-based catalysts and Ru-based catalysts [7–13]. The authors think that the reaction temperature of 600 °C is not enough to obtain higher performance of dry reforming, e.g., H_2 yields. According to previous studies using a Ni alloy catalyst as well as a Ru alloy catalyst, CH_4 conversion, H_2 yields, and H_2 selectivity increased with the increase in reaction temperature, and higher values were obtained over 600 °C [16,18–20]. To improve the performance of H_2 production and thermal efficiency, the following subjects can be considered: (i) the optimization of catalyst shape and composition, i.e., the pore size and weight ratio of Ni, Cr, and Ru, (ii) the optimization of the thickness and composition of the Pd/Cu membrane, i.e., a thinner membrane and a smaller ratio of Cu, and (iii) matching of the H_2 separation rate of the Pd/Cu membrane and the H_2 production rate of the catalyst, e.g., Ni/Cr/Ru, and deciding the optimum operation condition. They constitute the future work of this study.

4. Conclusions

In this study, we conducted an investigation to clarify the performance of a Ni/Cr/Ru catalyst used for a biogas dry reforming membrane reactor. In addition, in this study, we also undertook a comparison of the performance of the Ni/Cr/Ru catalyst with that of a Ni/Cr catalyst. The impact of operating temperature, the molar ratio of CH_4:CO_2, the differential pressure between the reaction chamber and the sweep chamber, and the introduction of a sweep gas on the performance of the biogas dry reforming membrane reactor using a Pd/Cu membrane and Ni/Cr/Ru catalyst was examined. As a result, the following conclusions can be drawn:

(i) It was revealed that the concentration of H_2 in the reaction chamber increases with the increase in the reaction temperature. This tendency is confirmed irrespective of the catalyst type as well as the differential pressure between the reaction chamber and the sweep chamber.

(ii) It was revealed that the concentration of H_2 in the sweep chamber increases with the increase in the reaction temperature. Since the concentration of H_2 in the reaction chamber is higher at higher reaction temperatures, the driving force to penetrate the Pd/Cu membrane is larger due to the high H_2 partial differential pressure between the reaction chamber and the sweep chamber. As a result, a higher concentration of H_2 in the sweep chamber was obtained.

(iii) It was revealed that the concentration of H_2 in the reaction chamber and the sweep chamber is higher with the decrease in the differential pressure. As to the differential pressure of 0.020 MPa, the differential pressure is too high, resulting in the separation rate of H_2 possibly being higher than the production rate of H_2 in the reaction chamber. As a result, it is thought that the effective non-equilibrium state cannot be obtained.

(iv) Regarding the effect of the sweep gas, since the amount of produced H_2 is not high, the driving force, i.e., the difference in partial pressure of H_2 between the reaction chamber and the sweep chamber, is not high. As a result, it is thought that the improvement in H_2 separation is not obtained by the introduction of the sweep gas.

(v) Comparing the performance of catalyst type, the concentration of H_2 in the reaction chamber and that in the sweep chamber using the Ni/Cr/Ru catalyst are much higher than those using the Ni/Cr catalyst. This tendency is confirmed irrespective of the reaction temperature and the differential pressure.

(vi) From the investigation in this study, the concentration of H_2 using the Ni/Cr/Ru catalyst is higher than that using the Ni/Cr catalyst by 2871 ppmV for the molar ratio of CH_4:CO_2 = 1.5:1 at the reaction temperature of 600 °C and the differential pressure of 0 MPa without a sweep gas in particular. The authors of this study think that the synergy effect of them was obtained.

(vii) It was revealed that the highest concentration of H_2 is obtained for the molar ratio of CH_4:CO_2 = 1.5:1 at 600 °C irrespective of the differential pressure and the catalyst type. The tendency that the highest concentration of H_2 is obtained for the molar ratio of CH_4:CO_2 = 1.5:1 among the investigated molar ratios matches with the authors' previous study investigating Ni and Ni/Cr catalysts.

(viii) According to the assessment evaluation, CO_2 conversion shows a negative value and the CO selectivity percentage is much higher than that of H_2 selectivity. The reaction mechanism can be explained as follows: (i) H_2 is produced by the reactions shown in Equations (1) and (5); (ii) the produced H_2 is consumed by the reaction shown in Equation (2), resulting in CO being produced; (iii) a part of CO produced by the reactions shown in Equations (1) and (2) is consumed during the reaction shown in Equation (6); and (iv) H_2O produced during the reactions of Equations (2) and (3) is consumed by Equation (4).

(ix) From the investigation in this study, the highest concentration of H_2 using the Ni/Cr/Ru catalyst was obtained for the molar ratio of CH_4:CO_2 = 1.5:1 at the reaction temperature of 600 °C and the differential pressure of 0 MPa without a sweep gas, which is 3080 ppmV. Under this condition, CH_4 conversion, H_2 yield, and thermal efficiency were 67.4%, 1.77 × 10^{-2}%, and 0.241%, respectively.

Author Contributions: Conceptualization and writing—original draft preparation, A.N.; methodology and data curation, M.I.; validation, S.Y. and R.I. All authors have read and agreed to the published version of the manuscript.

Funding: The authors acknowledge the financial support of the Iwatani Naoji Foundation, funding number of Iwatani Naoji Foundation is 42 and the joint re-search program of the Institute of Materials and Systems for Sustainability, Nagoya University.

Data Availability Statement: The original contributions presented in the study are included in the article, further inquiries can be directed to the corresponding author.

Conflicts of Interest: The authors declare no conflicts of interest.

References

1. Kalai, D.Y.; Stangeland, K.; Jin, Y.; Tucho, W.M.; Yu, Z. Biogas dry reforming for syngas production on La promoted hydrotalcited-erived Ni catalyst. *Int. J. Hydrogen Energy* **2018**, *43*, 19438–19450. [CrossRef]
2. World Bioenergy Association. Global Bioenergy Statistics. Available online: https://worldbioenergy.org/global-bioenergy-statistics (accessed on 2 April 2024).
3. The Japan Gas Association. Available online: https://www.gas.or.jp/gas-life/biogas/ (accessed on 2 April 2024).
4. Nishimura, A.; Takada, T.; Ohata, S.; Kolhe, M.L. Biogas dry reforming for hydrogen through membrane reactor utilizing negative pressure. *Fuels* **2021**, *2*, 194–209. [CrossRef]
5. Nishimura, A.; Hayashi, Y.; Ito, S.; Kolhe, M.L. Performance analysis of hydrogen production for a solid oxide fuel cell system using a biogas dry reforming membrane reactor with Ni and Ni/Cr catalysts. *Fuels* **2023**, *4*, 295–313. [CrossRef]
6. Nishimura, A.; Sato, R.; Hu, E. An energy production system powered by solar heat with biogas dry reforming reactor and solar heat with biogas dry reforming reactor and solid oxide fuel cell. *Smart Grid Renew. Energy* **2023**, *14*, 85–106. [CrossRef]
7. Tang, L.; Huang, X.; Ran, J.; Guo, F.; Niu, J.; Qiu, H.; Ou, Z.; Yan, Y.; Yang, Z.; Qin, C. Density functional theory studies on direct and oxygen assisted activation of C-H bond for dry reforming of methane over Rh-Ni catalyst. *Int. J. Hydrogen Energy* **2022**, *47*, 30391–30403. [CrossRef]
8. Rosset, M.; Feris, L.A.; Perez-Lopez, O.W. Biogas dry reforming using Ni-Al-LDH catalysts reconstructed with Mg and Zn. *Int. J. Hydrogen Energy* **2021**, *46*, 20359–20376. [CrossRef]
9. Moreno, A.A.; Ramirez-Reina, T.; Ivanova, S.; Roger, A.C.; Centeno, M.A.; Odriozola, J.A. Bimetallic Ni-Ru and Ni-Re catalysts for dry reforming of methane: Understanding the synergies of the selected promoters. *Front. Chem.* **2021**, *9*, 694976. [CrossRef]
10. Shah, M.; Mondal, P. Optimization of CO_2 reforming of methane process for the syngas production over Ni-Ce/TiO_2-ZrO_2 catalyst using the Taguchi method. *Int. J. Hydrogen Energy* **2021**, *46*, 22769–22812. [CrossRef]
11. Sharma, H.; Dhir, A. Hydrogen augmentation of biogas through dry reforming over bimetallic nickel-cobalt catalysts supported on titania. *Fuel* **2020**, *279*, 118389. [CrossRef]
12. Soria, M.A.; Mateos-Pedrero, C.; Guerrero-Ruiz, A.; Rodriguez-Ramos, I. Thermodynamic and experimental study of combined dry and steam reforming of methane on Ru/ZrO_2-La_2O_3 catalyst at low temperature. *Int. J. Hydrogen Energy* **2011**, *36*, 15212–15220. [CrossRef]

13. Andraos, S.; Abbas-Ghaleb, R.; Chlala, D.; Vita, A.; Italiano, C.; Lagana, M.; Pino, L.; Nakhl, M.; Specchia, S. Production of hydrogen by methane dry reforming over ruthenium-nickel based catalysts deposited on Al_2O_3 $MgAl_2O_4$ and YSZ. *Int. J. Hydrogen Energy* **2019**, *44*, 25706–25716. [CrossRef]
14. Nishimura, A.; Ohata, S.; Okukura, K.; Hu, E. The impact of operating conditions on the performance of a CH_4 dry reforming membrane reactor for H_2 production. *J. Energy Power Technol.* **2020**, *2*, 008. [CrossRef]
15. Cherbanski, R.; Kotkowski, T.; Molga, E. Thermogravimetric analysis of coking during dry reforming of methane. *Int. J. Hydrogen Energy* **2023**, *48*, 7346–7360. [CrossRef]
16. Kaviani, M.; Rezaei, M.; Alavi, S.M.; Akbari, E. Biogas dry reforming over nickel-silica sandwiched core-shell catalyst with various shell thickness. *Fuel* **2024**, *355*, 129533. [CrossRef]
17. Manfro, R.L.; Souza, M.M.V.M. Overview of Ni-based catalysts for hydrogen production from biogas reforming. *Catalysts* **2023**, *13*, 1296. [CrossRef]
18. Georgiadis, A.G.; Siakavelas, G.I.; Tsiotsias, A.I.; Charisous, N.D.; Ehrhardt, B.; Wang, W.; Sebastian, V.; Hinder, S.J.; Baker, M.A.; Mascotto, S.; et al. Biogas dry reforming over Ni/LnO_x-type catalysts (Ln = La, Ce, Sm or Pr). *Int. J. Hydrogen Energy* **2023**, *48*, 19953–19971. [CrossRef]
19. Martin-Espejo, J.L.; Merkouri, L.P.; Gandara-Loe, J.; Odriozola, J.A.; Reina, T.R.; Pastor-Perez, L. Nickel-based cerium zirconate inorganic complex structures for CO_2 valorisation via dry reforming of methane. *J. Environ. Sci.* **2024**, *140*, 12–23. [CrossRef] [PubMed]
20. Kiani, P.; Meshksar, M.; Rahimpour, M.R. Biogas reforming over La-promoted Ni/SBA-16 catalyst for syngas production: Catalytic structure and process activity investigation. *Int. J. Hydrogen Energy* **2023**, *48*, 6262–6274. [CrossRef]